IAC-17- C1.7.12

MISSION ANALYSIS FOR TWO POTENTIAL ASTEROIDS THREAT SCENARIOS: OPTIMAL IMPACT STRATEGIES AND TECHNOLOGY EVALUATION

C. Colombo [a], M. Albano [b], R. Bertacin [b], M. M. Castronuovo [b], A. Gabrielli [b], E. Perozzi [b], G. Valsecchi [c], E. Vellutini [b]

[a] *Dipartimento di Scienze e Tecnologie Aerospaziali, Politecnico di Milano, via La Masa 34, 20156, Milano, Italy* camilla.colombo@polimi.it
[b] *Italian Space Agency, via del Politecnico snc, 00133, Rome, Italy*, marco.castronuovo@asi.it
[c] *IAPS/INAF, IFAC/CNR, Via del Fosso del Cavaliere, 100, 00133 Roma RM, Italy, giovanni@iaps.inaf.it*

Abstract

The Space Mission Planning Advisory Group SMPAG's mission is to prepare for an international response to a Near Earth Object impact threat through the exchange of information, development of options for collaborative research and mission opportunities, and to conduct Near Earth Object (NEO) impact threat mitigation planning activities. This paper presents the preliminary work performed by the Italian Space Agency Delegation for defining few reference missions for different NEO-threat scenarios and carrying out Phase 0 studies. In this paper two scenarios are identified to study the possible response in case of a real NEO-threat. A direct and resonant impact scenario for an asteroid deflection mission are identified resembling to the asteroid 2010RF12 but with an increased asteroid mass. Then the mission analysis and spacecraft design for the direct impact case is performed and the results discussed.

Keywords: Near Earth Object, Near Earth Asteroid, Kinetic Impactor, Asteroid Deflection Mission.

Acronyms/Abbreviations

ASI	Italian Space Agency
DSM	Deep Space Manoeuvre
HGA	High Gain Antenna
IAWN	International Asteroid Warning Network
LGA	Low Gain Antenna
MAG	Absolute Magnitude
MOID	Minimum Orbit Interception Distance
NEA	Near Earth Asteroid
NEO	Near Earth Object
SMPAG	Space Mission Planning Advisory Group
SSPA	Solid State Power Amplifier
ADCS	Attitude Determination and Control System
TCS	Thermal Control System
TC/TM	Telecommand/Telemetry
GNC	Guidance and Navigation Control
TRL	Technology Readiness Level
TWTA	Travelling-Wave Tube Amplifiers
OBC	On Board Computer
FPGA	Field Programmable Gate Array
DH	Data Handling

1 Introduction

The Space Mission Planning Advisory Group (SMPAG) is a United Nation mandated group, constituted in 2014 following the recommendation of the working group on Near-Earth Objects (NEOs) and Technical Subcommittee of the United Nations Committee on the Peaceful Uses of Outer Space. In strong synergy with the International Asteroid Warning Network (IAWN), SMPAG's mission is to prepare for an international response to a NEO impact threat through the exchange of information, development of options for collaborative research and mission opportunities and to conduct NEO impact threat mitigation planning activities. The Italian Space Agency (ASI) is a member of SMPAG and contributes to the Group's activities.

Some works in literature analysed the efficiency of a kinetic impact mission on a general point of view [1]-[5]. The aim of those studies was to define a measure of efficiency that is not biased by the orbital parameters of a test-case object. In a work by Sanchez and Colombo [3], the ability of a small kinetic impactor spacecraft to mitigate an Earth-threatening asteroid was assessed by means of a measure of its efficiency. This measure estimated the probability of a space system to deflect a single randomly-generated Earth-impacting object to a safe distance from the Earth. A vast number of virtual Earth-impacting scenarios were investigated by homogenously distributing in orbital space a grid of almost 18,000 Earth impacting trajectories. The relative frequency of each trajectory was estimated by means of Opik's theory [6] and Bottke's near Earth objects model [7]. A design of the entire mitigation mission was performed and the largest deflected asteroid computed for each impacting trajectory. The results in [3] showed that current technology would likely suffice against discovered airburst and local damage threats, whereas

larger space systems would be necessary to reliably tackle impact hazard from larger threats. For example, it is shown that only 1,000 kg kinetic impactor would suffice to mitigate the impact threat of 27.1% of objects posing similar threat than that posed by Apophis.

In order to compliment those studies, rather than focusing on many different target asteroids, the approach followed within the SMPAG activity is to address few reference missions for different NEO-threat scenarios and carrying out Phase 0 studies.

Two scenarios are identified to study the possible response in case of a real NEO-threat, on the basis of the following criteria: (i) "Small-size" asteroid of 22 MAG corresponding to a diameter of 70 – 100 m, direct impact trajectory, lead time to impact of about 10 years; (ii) "Large-size" asteroid 17 MAG corresponding to a diameter of 500 m – 1 km, resonant encounter trajectory, lead time to the impact of about 20 years. In both cases the asteroid 2010RF12 was chosen as a representative target, as currently it has the highest probability of hitting the Earth. As this asteroid's diameter is only between 4 m and 12 m, its orbit was used in this study, while its size was increased to create a synthetic object. Indeed, 2010RF12's orbit will lead to either an impact with the Earth, or a very close encounter with it, at the end of the current century.

The paper focuses on the first asteroid scenario, which results in a direct impact with the Earth. The deflection strategy of the NEO's impacting trajectory is selected by means of an optimisation procedure developed in [2] to minimise the spacecraft launch mass, while maximising the asteroid miss distance. To get significant advances in the verification of the technical feasibility of the deflection strategy identified, the analysis will define all the mission components, from the launcher identification to the design of the spacecraft system and subsystems (e.g. propulsion, power management, GNC etc.).

The paper is organised as follows. Section 2 explains the rationale behind the synthetic asteroid selection, Section 3 describes the design of the deflection strategy, whose results are described in Section 4. A preliminary spacecraft design is performed in Section 5. Finally, Section 6 describes the future works within the SMPAG framework.

2 Target asteroid selection

The asteroid selected for this study is a synthetic asteroid that resemble for many characteristics the NEO 2010 RF12. 2010 RF12 is a small Near Earth Asteroid (NEA); its absolute magnitude H is 28.4, corresponding to a diameter between 4 m and 12 m. Currently, it has the highest probability of hitting the Earth: in both the risk pages of NEODyS-2 [8] and of Sentry [9] the impact probability is estimated to be around 6% for an impact on 5.99 September 2095. The energy liberated by such an impact will be of the order of, or somewhat less than, the energy of the Hiroshima bomb, and the collision will generate an airburst comparable to those that take place about once per year on our planet and in most cases are recorded only by infrasound sensors. 2010 RF12 was discovered on 5 September 2010, and observed for 3 days, until 8 September, during a close encounter with the Earth that brought it, on 8 September, within 79,400 km from the centre of the Earth.

2.1 Orbital evolution

Before the discovery encounter 2010 RF12 moved on an orbit with a = 0.997 AU, e = 0.176, i = 3.55 deg, Ω = 165.7 deg, ω = 284.0 deg. The Earth encounter changed the orbital parameters of the NEA, and the orbit of 2010 RF12 is currently characterised by a = 1.060 AU, e = 0.188, i = 0.88 deg, Ω = 163.8 deg, ω = 267.6 deg. Between the current epoch and the September 2095 potential impact, 2010 RF12 undergoes a number of encounters with the Earth, none of which changes the orbit appreciably, with the partial exceptions of two shallow encounters, one in February 2059, that changes the orbit into a = 1.057 AU, e = 0.187, i = 0.90 deg, Ω = 163.0 deg, ω = 266.9 deg, and another one in February 2084, that slightly modifies the orbit into a = 1.057 AU, e = 0.187, i = 0.91 deg, Ω = 162.8 deg, ω = 267.1 deg; it is in this orbit that 2010 RF12 encounters, and possibly impacts, the Earth in 2095.

NEAs move on a wide variety of orbits; therefore any particular choice can be considered as not particularly representative of the whole population. On the other hand, the orbit of 2010 RF12 will lead to either an impact with the Earth, or a very close encounter with it, at the end of the current century; therefore, it can be considered a "realistic" impactor orbit, and is as good as any other NEA impact orbit for the study of a deflection mission.

2.2 Direct hit and resonant return hits

For both NEODyS and Sentry the 2095 collision is for the nominal orbit or very close to it; thus, the currently available data can be taken as representative of a direct hit, since the 2059 and 2084 shallow encounters do not change the orbit significantly. If, instead, we assume that in 2095 2010 RF12 will miss the Earth – an assumption largely compatible with the current observational record – the Earth encounter will spawn a very large number of resonant returns, among which suitable orbits to simulate the deflection in case of resonant returns can be chosen. In addition to the above possibilities, the relatively long interval of time between now and 2095 allows to simulate the acquisition of further observational data, in order to model a realistic

increase of the knowledge of the asteroid orbit and of its physical properties in the years preceding the impact.

In this respect, simulation scenarios should involve a fictitious asteroid with the same orbit as 2010 RF12, but, to consider a real threatening scenario, with the absolute magnitude H increased by, e.g.:

- 5, so that H = 23.4; this would raise the energy liberated at collision to something of the order the Tunguska event, and would make the asteroid detectability easier at pre-2095 apparitions;
- 10, so that H = 18.4; this would raise the energy liberated at collision to something of the order of many thousands of megatons, and would make the asteroid detectability much easier at pre-2095 apparitions.

Following previous considerations, Table 1 and Table 2 summarise the characteristics of the NEO assumed respectively for the direct hit scenario and the resonant one. In this article, however, only the direct scenario will be analysed.

Table 1. NEO parameters assumed in the direct hit scenario.

Reference diameter	**100 m**
Magnitude	21÷20
Mean density	2600 kg/m^3
Estimated Total Mass	1.3614 x 10^9 kg
Detection Time	2085
Expected Impact Time	2095
Type of impact	Direct hit
Orbital parameters	as 2010RF12

Table 2. NEO parameters assumed in the resonant hit scenario

Reference diameter	**1000 m**
Magnitude	17÷18
Mean density	2600 kg/m^3
Estimated Total Mass	1.3614 x 10^{12} kg
Detection Time	2085
Expected Impact Time	fill
Type of impact	Resonant hit
Orbital parameters	as 2010RF12

3 Deflection strategy design

The configuration of the direct impact scenario is shown in Figure 1.

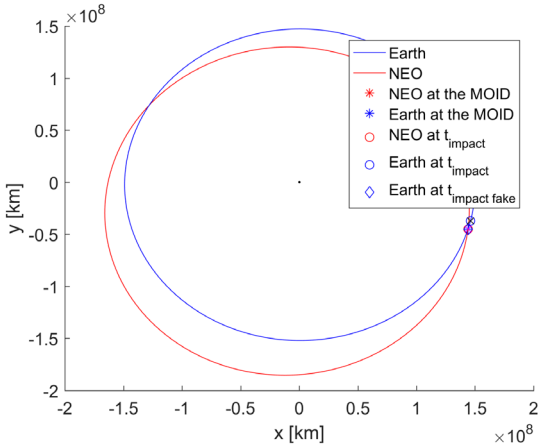

Figure 1. Earth and NEA trajectory.

As the expected impact time is set to 2095 and we assume the asteroid to be detected 10 year in advance (see Table 1), the minimum starting time for the deflection mission is assumed to be at

$$t_{0,\min} = t_{MOID} - 10 \text{ years}$$

where t_{MOID} is the time where the asteroid will be a the Minimum Orbit Interception Distance (MOID) with the Earth in 2095 The design parameters for the asteroid deflection mission are the time of departure and the Δv at departure in magnitude and direction, the time of flight, the timing and magnitude of a Deep Space Manoeuvre (DSM) to adjust the spacecraft trajectory and the initial mass of the spacecraft. An optimisation problem similar to the one in [1] and [2] was set to find the optimal design of the parameter vector x:

$$x = \left[\eta_{t_0} \quad \eta_{DSM} \quad ToF \quad \Delta v_0 \quad \alpha_0 \quad \delta_0 \quad m_{s/c0}\right]$$

where ToF is the time of flight for the interplanetary trajectory, from departure from Earth to the asteroid interception, Δv_0 is the magnitude of the delta velocity at departure from Earth, while α_0 and δ_0 are the in-plane and out-of-plane angles with respect to the heliocentric velocity of the Earth. $m_{s/c0}$ is the wet mass of the spacecraft at launch, η_{t_0} is used to define the departure date of the spacecraft from Earth as:

$$t_0 = t_{0,\min} + \left(t_{MOID} - t_0 - ToF\right)\eta_{t_0}$$

A deep space manoeuvre is also performed at a fraction η_{DSM} of the time of flight, where η_{ToF} is a value between 0 and 1, so that if η_{DSM} =0 no DSM is performed. The magnitude and direction of the DSM are determined solving a Lambert problem from the DSM point at time

$$t_{DSM} = t_0 + \eta_{DSM} ToF$$

to the asteroid position at time

$$t_{deflection} = t_0 + ToF \ .$$

The design parameter vector x need to be determined such that it minimises the two-criteria objective function:

$$J = \left[m_{sc0} \quad \Delta r_p \right]$$

where m_{sc0} is the spacecraft mass at launch, that is taken as a measure of the cost of the mission, while Δr_p is the radius of the perigee at the hyperbolic passage of the asteroid from Earth during the close approach of 2095. From the Lambert arc, the final velocity of the spacecraft at its encounter with the asteroid can be calculated and from it the delta velocity imparted to the asteroid via kinetic impact can be computed as:

$$\delta v_{NEA}\left(t_d\right) = \beta \frac{m_{sc,d}}{m_{NEA} + m_{sc,d}} \Delta v_{s/c}\left(t_d\right) \qquad (1)$$

where $\Delta v_{s/c}$ is the relative velocity of the spacecraft with respect to the asteroid at the impact point, and the parameter β has a value of 1 in this implementation.

The deflection of the asteroid is calculated at the time of its nominal passage from the MOID with the Earth orbit via the use of relative motion equation and Gauss planetary equations written for finite differences [2] so that

$$\delta \mathbf{r}\left(t_{\text{impact}}\right) \approx \mathbf{\Phi}\left[t_{\text{impact}}, t_d\right] \delta \mathbf{v}\left(t_d\right)$$

where $\mathbf{\Phi}\left[t_{impact}, t_d\right]$ is the transition matrix defined through the proximal motion equations and Gauss's planetary equations. The deflection $\delta \mathbf{r}\left(t_{\text{impact}}\right)$ is then translated into the impact parameter b^* on the b-plane [6], which describes the minimum intersection distance between the deflected asteroid and the Earth, through a matrix rotation described in [2]. Furthermore, the effect of the Earth's gravity on the deflected trajectory of the asteroid is taken into account by including the hyperbolic factor:

$$r_p = \sqrt{\frac{\mu_\oplus^2}{v_\infty^4} + b^{*2}} - \frac{\mu_\oplus}{v_\infty^2} \qquad (2)$$

where $v_\infty = \left(\mathbf{v}_{NEA} - \mathbf{v}_{\text{Earth}}\right)$ is the relative velocity of the asteroid with respect to the Earth as given in Eq. (1).

4 Mission analysis and design

4.1 Launcher selection

The launcher will be able to inject the satellite on the escape orbit. The Δv provided by the launcher is partially used for the first manoeuvre to inject the satellite in its interplanetary trajectory to reach the asteroid and impact with it.

Considering the mass of the impactor and the declination required with respect to the equatorial plane, a solution could be the use of a Proton M which can give the widest and highest opportunity of launch.

The launcher capacity for earth escape mission, which depends on the launcher payload mass is reported in the diagram in Figure 2 and has been used for the calculations [13].

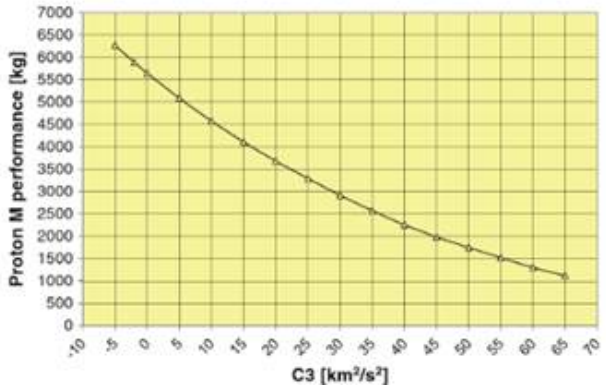

Figure 2. Launch capacity for Earth escape missions for Proton [13].

4.2 Parametric analysis

The results of the optimisation described in Section 3 are presented in the following. Here the departure Δv is not entirely given by the spacecraft but the launcher is assumed to provide a relative escape velocity of 3 km/s in a free direction in the ecliptic plane that is determined by the optimiser. Figure 3 contains a sample of the optimal trajectories as a result of the minimisation of the two value cost function reported in Figure 4, namely the wet mass at launch and the impact parameter b^*. The mass ratio $m_p / m_{sc,0}$ associated to the transfer trajectory is represented in Figure 5. The designed trajectory results in a deflection at the asteroid which is characterised in Figure 6 to Figure 8; Figure 6 indeed represents the $\delta v_{NEA}\left(t_d\right)$ imparted at the asteroid versus the achievable distance displacement at the MOID, Figure 7 describes the direction of the $\delta v_{NEA}\left(t_d\right)$ direction imparted to the asteroid. As the transfer phase and the deflection phase are optimised simultaneously, the deflection manoeuvre is not completely in the anti-tangent direction, but has a small non-negative out-of-plane component β. The effectiveness of the manoeuvre can be represented in Figure 8 which shows the warning time versus the achievable deflection.

As it can be seen from Figure 6 to Figure 8, the mission via kinetic impactor is not sufficient to deflect the asteroid by a safe distance higher than the Earth-Moon distant. Due to the high mass of the spacecraft and the relatively short warning time the effective deflection with respect to the nominal case is only of about 6000 km (around one Earth radius). This is in agreement with previous studies on the kinetic impactor

that shows that for a warning time of less than 10 years and masses of 100 kg of above, the efficiency of the kinetic impactor is strongly dependent on the orbit, i.e. elliptical orbit are easier to be deflected. Moreover, as the deflection is given after the close encounter with the Earth, the gravitational pull of the Earth cannot be exploited to increase the deviation of the NEO at the following close approach.

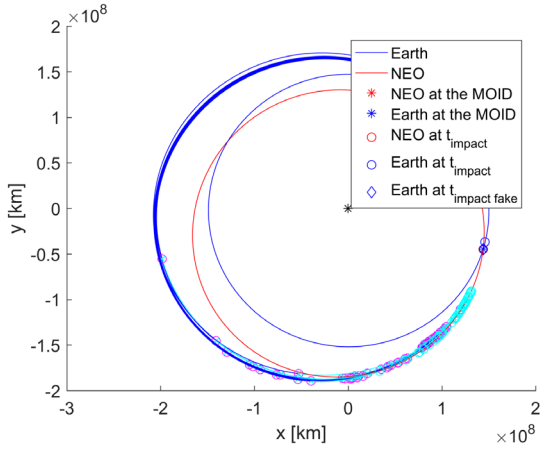

Figure 3. Sample of deflection trajectories.

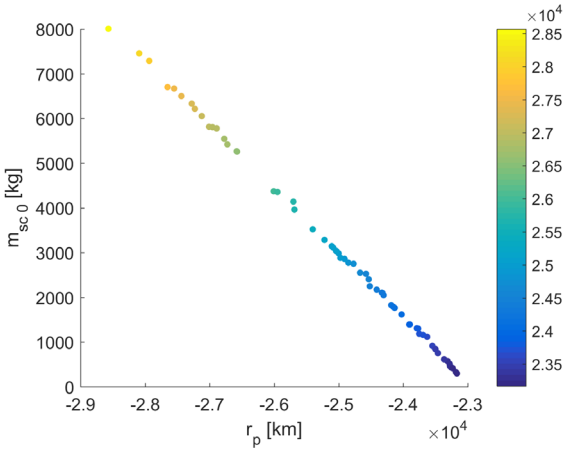

Figure 4. Spacecraft initial mass as function of the achievable deflection at the MOID.

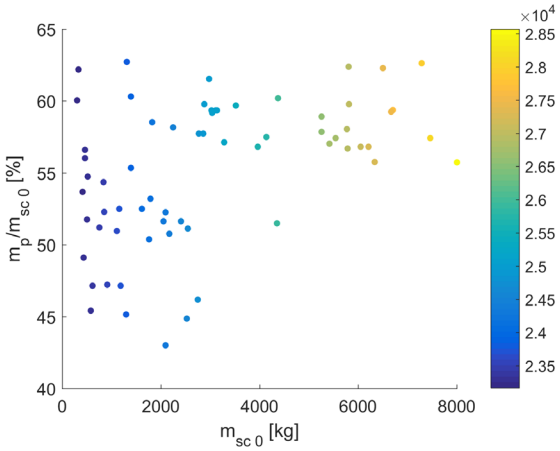

Figure 5. Spacecraft initial mass vs propellant mass ratio.

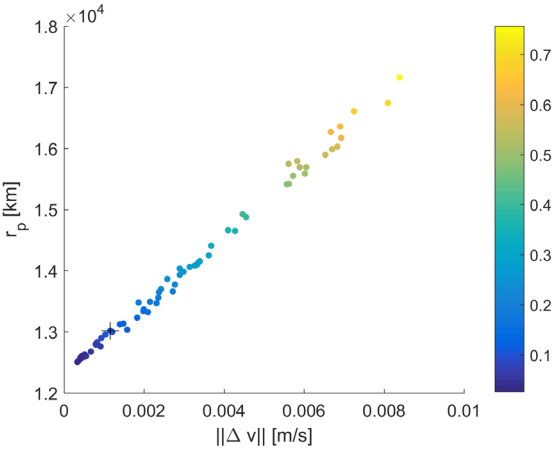

Figure 6. Delta velocity imparted at the asteroid vs achievable deflection (colour bar deflection success).

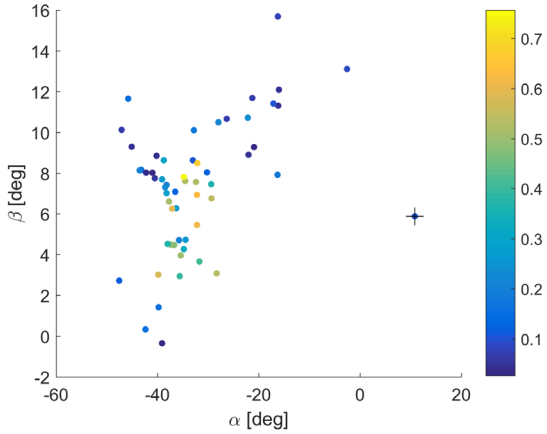

Figure 7. Direction of the deflection manoeuvre applied to the asteroid.

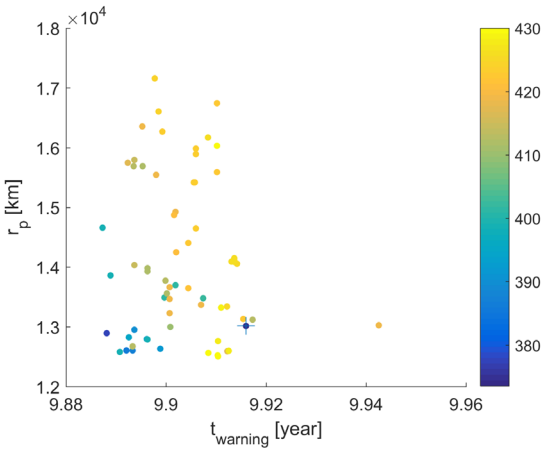

Figure 8. Warning time vs achievable deflection.

5 Spacecraft design

5.1 Spacecraft requirements

Unlike traditional spacecraft devoted to science, e.g. to solar system exploration, the goal of the kinetic impactor is to be as massive as possible when reaching the NEO target, in order to maximize the deflection result.

For this reason, the spacecraft essentially hosts no scientific payload, except the instrumentation used for NEO imaging and targeting and relative data acquisition and processing. Moreover, its configuration carries essential subsystems in order to make it as feasible and easy-to-integrate as possible. Redundancies in critical components, such as in the imaging equipment, could be considered to increase the robustness of such mission.

High TRL technologies, i.e. with a TRL-7 as minimum, have been considered, to reduce the time required by the spacecraft development phase, gathering most of its components from previous mission designs or directly from available commercial off-the-shelf equipment.

The preliminary design of the spacecraft has been carried out considering the following requirements and assumptions:

SC-Req 01. The spacecraft shall be able to perform autonomously the navigation toward the asteroid and the final targeting of the impact point by use of OBC and high resolution images;

SC-Req 02. The spacecraft shall be able to operate at a maximum distance of 1.5 AU from the Sun;

SC-Req 03. The spacecraft shall be able to communicate with Earth at a maximum distance of 2 AU;

SC-Req 04. Low cost technologies with a TRL ≥ 7 shall be adopted for the spacecraft design and integration;

SC-Req 05. The spacecraft shall be configured in order to assure a high level of AOC performances, mainly in the targeting and approaching phase

The typical spacecraft subsystem tree is reported in Figure 9.

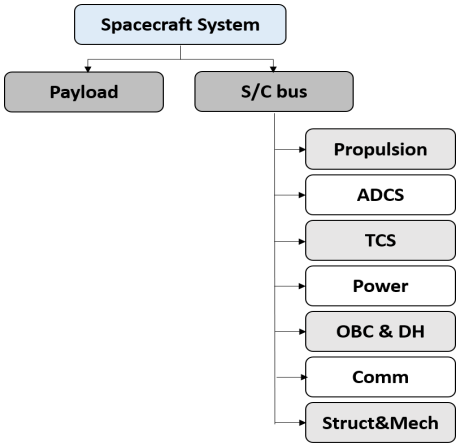

Figure 9. Spacecraft subsystems tree.

5.2 Payload

As already mentioned above, given the specific mission objective, which is the deflection of a NEO from its Earth-impacting trajectory, the only payload hosted on-board are instruments devoted to the asteroid imaging and the optical S/C navigation.

Given the large distances between the S/C and the Earth, as in most of the interplanetary missions, real-time navigation and guidance is performed on-board with a high degree of autonomy. This is particularly required during critical events, such as the target approach phase preceding the impact of the spacecraft, when the transmission time delay with the Operations Control Center would make orbit determination and guidance on the ground useless. Traditional orbit determination by means of DDOR technique, can performed during the cruise phase when the orbit correction manoeuvres can be planned some time in advance. DDOR makes use of the on-board telecommunication sub-system and no ad-hoc apparatus is needed for this function.

For the real-time navigation and guidance, instead, a suitable optical camera and data processing system are essential on board. As an example, in 2005 the impactor released by the Deep Impact NASA probe carried a

targeting camera that was successfully used for the final guidance phase towards the comet Tempel 1.

This spacecraft will navigate by using optical data taken by the onboard camera to determine its orbit, and use this information to predict its future trajectory and make necessary course corrections. The basic navigation data available from the camera are star-relative astrometric observations of solar system bodies which can be used to determine line-of-sight vectors to those objects and particularly to the target asteroid.

Off-the-shelf optical systems with the required performances are presently available and can be considered in the proposed mission. The spacecraft is equipped with two cameras, a wide-angle medium resolution instrument and a high resolution instrument with a quite narrower field of view. A laser altimeter, usually called light detection and ranging (LIDAR), like the one mounted on-board of Hayabusa 2 S/C, can be used for the final approach.

For what concerns the wide-angle camera, a good reference is given by the Wide Angle Camera (WAC) that is going to be mounted on ExoMars Rover 2020, whose main characteristics are contained in Figure 3.

Table 3. Parameters of the Wide Angle Camera that is going to be mounted on ExoMars Rover 2020.

Parameter	
FOV (°)	38.3 x 38.3
Pixels	1024 x 1024
Filter type	Multispectral Filter Wheel
Filter number	11
IFOV (mrad/pixel)	653
Pixel scale (2 m)	1.31 mm
Focus	Fixed (1.0 m to ∞)
Mass	2.13 kg (including margin)
Power	3.4–9.2 W (including margin), depending on operating mode

As a reference high resolution camera, the ECAM-C50 produced by Malin Space Science Systems (USA) has been considered. A Digital Video Recorder (DVR) commands the camera, pre-processes and compresses the data, and stores the data to a non-volatile memory buffer (available with 8, 16, or 32 GBytes of memory). Table 4 the relevant characteristics.

Table 4. Parameters of the high resolution camera, the ECAM-C50 produced by Malin Space Science Systems. Courtesy of MSSS, San Diego CA, USA. www.msss.com

Parameter	**ECAM-C50**	**ECAM-DVR4**
Mass (without optics)	256 g	1110 g
Dimensions	78(W) x 58(L) x 44(H) mm	183(W) x 157(L) x 32(H) mm
Power Consumption	1.75 W (idle) 2.5 W (imaging)	9.75 W (idle) 13.5 W (imaging)
Focal Plane	CMOS, 5 Megapixel (2650 x 1944 pixels)	
Wavelength range	400 nm - 750 nm	
Imaging modes	Monochrome or RGB using Bayer Pattern Filter	
Narrow FOV Optic	FOV 25°(H) x 19°(V): Focal Length 12.6 mm; f/3.5	
Medium FOV Optic	FOV 44°(H) x 35°(V): Focal Length 7.1 mm; f/3.5	
Wide FOV Optic	FOV 77°(H) x 55°(V): Focal Length 4.7 mm; f/3.5	
Frame size	Full 2650 x 1944, WQXGA 2560 x 1600, QXGA 2048x1536, HD1080p 2048x1080, HD720p 1280x720, VGA 640x480	
Frame rates	Full 3 frame/s, WQXGA 3.5 frame/s, QXGA 2.5 frames/s, HD1080p 4 frames/s, HD720 8 frames/s, VGA 20 frames/s	
On-board Storage (DVR)	8, 16, or 32 GBytes	
Image Compression (DVR)	JPEG (Lossy), First-Difference Huffman (Lossless)	

5.3 Spacecraft subsystems

Unlike traditional satellites, in our case the sizing of the bus subsystems is not directly linked and derived from the required payload in terms of mass and power budgets, but depends on the mass required at the impact with the NEO. In this preliminary phase, no detailed definition of the layout of each subsystem is possible, even if existent basic components are selected, since the specific arrangement and inter-connection will be imposed by the overall system layout.

Hence, a statistical approach has been adopted on the base of previous missions and literature analyses [10], assuming suitable margins to account for uncertainties and possible additions.

The main inputs considered for the spacecraft sizing have been obtained from the trajectory analysis, namely the total Δv required to perform the orbital transfer and the final spacecraft mass immediately before the impact with the NEO.

A margin of 25% has been applied to the mass and power estimated budgets, in order to consider uncertainties related to such preliminary design phase, as commonly assumed in typical sizing procedures [10].

5.3.1 Propulsion subsystem

A chemical propulsion system has been chosen due to its high reliability which arise from the long heritage. In particular, a Hydrazine monopropellant propulsion system has been selected. The propellant quantity is defined directly through the trajectory optimization by use of the classical Tsiolkovsky equation, which anyway assumes the propulsive action as impulsive, i.e. with infinitesimal duration. This propellant amount is

defined on the basis of the final impactor mass and the required Δv manoeuvres during the transfer towards the NEO (one manoeuvre to leave Earth gravity field and a second one in deep space to reach the final trajectory). As stated in literature [10], a margin of 20% is generally considered (in terms of extra Δv) to deal with contingencies. This margin can be converted in terms of "extra propellant mass" resulting in an average value of 12%. The mass of the tanks is included in the structures total mass.

A possible candidate engine model, reported in the following table, has been already used for Planck, Herschel and METOP 1 missions. Taking into account the impactor mass and Δ*v* required, a cluster of 12 thrusters have been considered appropriate.

Table 5. 20 N class Engine characteristics [11]

Parameter	Nominal value
Nominal Isp	222-230 s
Mass	650 g (x 12)
Propellant type	Monopropellant, hydrazine
Total operating time	10.5 h

The power consumption data are not available; thus it is linearly derived from a generic 1.5 N class thruster which consumption is of 6W. Then the average power consumption is of 70 W for each thruster.

5.3.2 ADCS subsystem

The Attitude Determination and Control subsystem sizing depends on the mass amount and mass distribution of the S/C. However, in this very preliminary design phase, this dependency can be considered weak. This means that the range in the ADCS subsystem mass can be considered already included in its margin.

For attitude determination the S/C uses star-trackers. This technology is reliable, employed in most of this type of missions, it has not high costs and it is lightweight. As reference star sensor the product VST-68M of the German company Vectronic Aerospace has been considered.

Table 6. Star sensors characteristics (Courtesy of VECTRONIC Aerospace GmbH, http://www.vectronic-aerospace.com/).

Mechanical	
Dimensions (with baffle)	60 x 60 x 138 mm
Mass	0.470 kg
Mounting pattern	4 x M4 50 x 90 mm
Electrical	
Power consumption, max	3.0 W
Input voltage range (VCD)	9 to 40
Environmental	
Operating temp.range	-20°C to + 65°C
Storage temp. range	-40°C to + 80°C
Vibration	20g rms random 3 axis
Radiation tolerance	> 20 krad
Performance	
Accuracy 2σ (x, y / z axis)	5 arcsec / 30 arcsec
Acquisition probability	> 99.7%
Update rate	5 Hz
Field of view	14° x 14°
Time of first acquisition	typ. 1 sec

The pointing control is guaranteed by a system with full redundancy. In particular, four reaction wheels are foreseen in a skewed configuration for 3-axis control. In addition, hydrazine-based thrusters are provided for wheels desaturation and for redundancy in case of wheels failure.

A possible example of last generation reaction wheel employed by Jaxa for medium size spacecraft (will be launched on GOSAT-2 2018) is shown in the following table.

Table 7. Reaction wheels characteristics [12].

Item	Specification
Momentum (Max.)	30 Nms
Output torque (Max)	-6000 rpm ~ +6000 rpm
Run-up time	25 s ~ 150 s
Coast-down time	238 s ~ 738 s
Power consumption	
Peak torque	<230 W
Steady state	18 W ~ 35 W
Mass	5 kg

Hydrazine thrusters come from ArianeGroup heritage. The following table shows the characteristics of 1N thrusters suitable for this type of high precision attitude control (already tested for Cosmo Skymed and Sentinel satellites).

Table 8. 1-N Hydrazine thruster characteristics [11].

Characteristics	Values
Thrust, Nominal	1N
Thrust Range	0.320 - 1.1N
Specific Impulse, Nominal	220 s
Propellant	Hydrazine (N2H4), High Purity Grade
Total Impulse	135,000 Ns

5.3.3 TCS subsystem

Thermal blankets, also referred to as multilayer insulation, are used on the spacecraft to insulate thermally against radiative heat transfer. They are used in such applications as insulation against solar heating and against heat transfer from hot motors and exhaust plumes. They can also serve as a thermal barrier during the launch phase when the spacecraft is no longer protected by the launch vehicle payload shroud. Thermal blankets are used not only to reduce heat gain but also to reduce heat loss. Particularly in deep-space missions, electric heating of key components may be needed. The application of MLI then reduces the need for electric power. MLI are usually composed by a number of layers, most often aluminized Mylar of Kapton, typically 20 to 30 μm thick. For higher temperatures, up to 340°C, Kapton is preferred over the cheaper Mylar.

The heater mass is less than 100g. The design foresees also the use of MLI, which are lightweight structures, their total mass being dependant on the total surface they cover. The use of radiators does not seem necessary.

The thermal control system (TCS) is the largest consumer of power for Earth satellites. In our case, however, the TCS architecture is much simpler and less demanding in terms of power consumption.

5.3.4 OBC & DH subsystem

Considering the very high level approach adopted for the S/C sizing process, it is not feasible, in the present stage, to size exactly the OBC and DH subsystem, since it strictly depends on the global configuration and complexity of the spacecraft, e.g. on housekeeping sensors set, data bus characteristics, the amount of telemetry or payload data to be transmitted and so on.

Given the large distances between the S/C and the Earth, as in most of the interplanetary missions, real-time navigation and guidance is performed on-board with a high degree of autonomy. This is particularly required during critical events, such as the target approach phase preceding the impact of the spacecraft, when the transmission time delay with the Operations Control Centre would make attitude and orbit determination and guidance on the ground useless. Hence, high performance on-board subsystems for data processing and for the implementation of S/C guidance and control are required. On the other side, since scientific goals are not of primary importance, data storage needs are expected to be limited.

On the basis of the previous considerations, a medium complexity of the system could be assumed and, referring to [10], an overall estimation in terms of mass and power absorbed can be performed.

Considering, for simplicity, a single combined subsystem, in which both command and TM processing are performed, an overall mass of about 12 kg (including 25% margin) is estimated and a nominal power consumption of about 19 W (including 25% margin) can be considered.

Redundancy of critical components, e.g. FPGA boards, is mandatory in order to guarantee the necessary fault tolerance level for the mission achievement.

5.3.5 Communication subsystem

A required maximum operative distance of 2 AU from the Earth has been assumed for the sizing of TC/TM subsystem and the choice of transmission carrier.

An X-band transmission system has been selected both for uplink and downlink communications, normally adopted for deep space missions. Due to the higher downlink data rate expected, this capability has been analysed in detail for the subsystem sizing.

20W has been considered as a reasonable output transmitting power for the downlink data transmission (@ 8.4 GHz), which is in line with the technical heritage from previous missions operating at similar distances (e.g. Mars exploration).

A main 1.5m-diameter parabolic HGA, similar to those adopted in Hayabusa or Deep Impact missions, with a peak gain of about 40 dB has been considered for the sizing. An auxiliary LGA, usually mounted on top of LGA sub-reflector, has been included in the mass budget estimation for redundancy, mainly for uplink TC reception.

The mass of the communication subsystem, including antenna, feed, receiver, and supporting structures, depends largely on its configuration and the materials used. However, coupling the HGA-LGA configuration with a typical SSPA transmitter results in an overall mass budget estimation of about 25 kg (including 25% margin) and a nominal power consumption of about 90 W (including 25% margin).

Even if autonomous navigation and NEO targeting capabilities are required from the spacecraft, a transmission of compressed images to the Ground Station is foreseen in order to perform detailed morphological and mass/volume analysis of the target, to better define the impact parameters. Considering the heritage of previous mission and studies (e.g. Deep Impact, Don Quijote), a downlink data rate of the order of the 1 Mbps has been assumed for the present stage, with a transmission peak in the final phases before the impact. A TC data rate of the order of 1 kbps has been, instead, assumed for the uplink transmission.

5.3.6 Power subsystem

On the basis of the power needs from the other spacecraft subsystems (Table 3), a preliminary overall average power consumption of about 800 W has been estimated, which is in line with the values featured in other similar missions.

Table 9. Spacecraft subsystems power budget estimations.

SUBSYSTEM	AVERAGE POWER (W)
PROPULSION	420
AOCS	40
THERMAL	250
PAYLOAD	20
COMMUNICATION	90
OBC & DH	19
TOTAL	**~800**

A peak power consumption of about 1600 W (@ 28V bus voltage), mainly referred to the targeting and approach phases, has been derived considering a simple factor 2, in order to size the primary power source.

Considering the maximum required operative distance from the Sun (1.5 AU) a typical solar array solution has been considered. Furthermore, given the high level of pointing accuracy required to the spacecraft, a compact configuration is preferred by using short deployed appendages, e.g. with main dimension aligned with spacecraft axis.

Considering the worst case conditions, referred to the maximum Sun distance of 1.5 AU, corresponding to a minimum solar flux of ~600 W/m^2, and typical efficiencies (e.g. gallium/arsenide solar cells), an overall illuminated array area of about 33 m^2 has been obtained.

A secondary rechargeable power source has also been included in the analysis for peak loading phases and for emergency conditions, considering as reference a nickel-hydrogen (Ni-H_2) technology and a battery capacity of 15 amp-hr or 420 W-hr. Concluding, a final mass budget of 190 kg (including a 25% margin) has been assumed for the whole power generation and control, regulation and storage subsystem.

5.3.7 Structure and mechanisms

Structures and mechanisms mass of spacecraft has historically been evaluated to consist in only about 20% of the total dry mass. However, in our case a consistent percentage of the total S/C mass can be considered constituted by "ballast", necessary to reach the needed impact deflection effect.

Such residual mass can be balanced by equipping the S/C with further optical payloads (with of course an impact on some of the other subsystems) or by stiffening the S/C structure, in order to limit the kinetic energy loss due to the collapsing of the S/C bus (as stated by the impacts' theory).

Main objective of present sizing activity has been the preliminary evaluation of this available mass margin, increasing the required spacecraft mass, postponing to a future detailed activity the analysis of its best allocation.

Figure 10 shows a schematic representation of assumed mass budget distribution, highlighting this distinction between the basic spacecraft subsystems/structures and the residual "inert" mass.

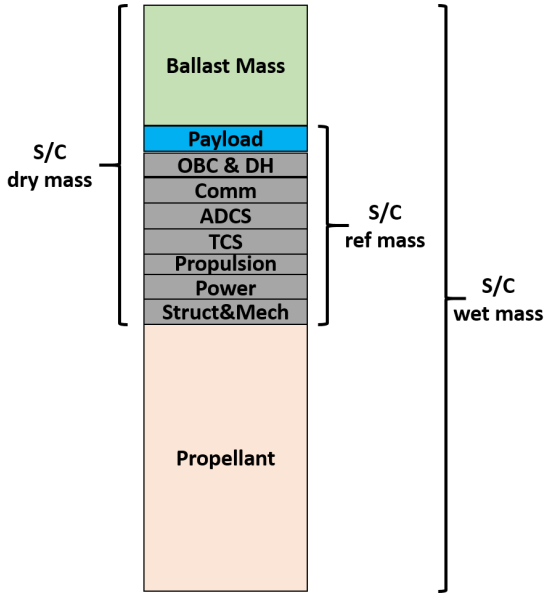

Figure 10. Spacecraft mass budget definitions.

5.3.8 Ballast Mass

Optical payload and S/C subsystems (included structures and mechanisms) are indicated for convenience as dry "reference mass" of the S/C to perform its operative functions and achieve the mission goals: this mass budget is the minimum needed for the integration of the satellite.

Following considerations mentioned in previous paragraphs, such reference mass could be considered almost constant, except the structures' fraction which are linearly dependent to the overall S/C dry mass.

Table 10 summarises final results of the preliminary sizing of S/C subsystems, to be used in the ballast percentage calculation.

Table 10. Preliminary results of S/C subsystems mass budget estimation.

	Max. Value (including 25% margin) [kg]
Payload	12.5
S/C Subsystems	**279**
ADCS	25
OBC&DH	12
Power	190
Propulsion	17
Thermal	10
TT&C (Comm)	25
Structures & Mechanisms	20% of S/C dry mass

Starting from the wet mass amount (Fig. 9), foreseen by the NEO deflection analysis and trajectory optimization, the overall dry mass has been computed by subtracting the required total propellant mass for orbital manoeuvres, (considering also the margin previously introduced). Finally, ballast mass is computed by simply subtracting the payload and subsystems reference mass from the obtained S/C dry budget.

Figure 11 and Figure 12 show the percentage relation between this ballast mass amount and respectively the S/C overall dry and wet masses.

As expected, this addictive mass availability quickly decreases moving toward lighter S/Cs to reach a "saturation" condition, corresponding to the subsystems reference mass, while assumes an asymptotic trend toward heavier S/C masses. Considering mission requirements discussed in Section 4.2, the minimum feasible S/C dry mass is about 370 kg, which corresponds to about 840 kg once equipped with the propellant amount needed to perform the required orbital transfer.

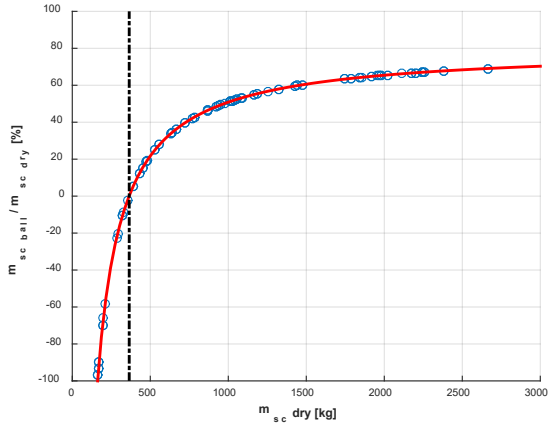

Figure 11. Ballast mass percentage as function of S/C dry mass.

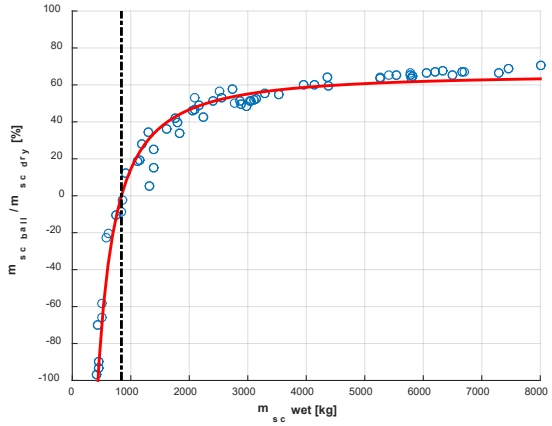

Figure 12. Ballast mass percentage as a function of S/C wet mass.

6 Conclusions

This paper presented the preliminary design of a representative deflection mission to a synthetic Near Earth Asteroid that is chosen similar to the object 2010RF12 but with an increased mass so that $H = 23.4$. The optimal transfer trajectory with one deep space manoeuvre has been designed to minimise the initial wet mass at launch and the asteroid displacement at the MOID. The effects of uncertainties in the deflection manoeuvre and the asteroid's response to the deflection action will be taken into account in a future work.

Acknowledgements

The authors would like to acknowledge Dr. Pierluigi Di Lizia for his comments ad discussion on the work. C. Colombo the European Research Council (ERC) starting grant COMPASS (grant agreement No 679086 – COMPASS), under the European Union's Horizon 2020 research and innovation programme.

References

[1] Izzo D., "Optimization of interplanetary trajectories for impulsive and continuous asteroid deflection", Journal of Guidance, Control and Dynamics Vol. 30, 2007, pp. 401–40

[2] Vasile M., Colombo C., "Optimal Impact Strategies for Asteroid Deflection", Journal of Guidance, Control, and Dynamics, Vol. 31, No. 4, Jul.–Aug. 2008, pp. 858-872, doi: 10.2514/1.33432.

[3] Sanchez J. P., Colombo C., "Impact hazard protection efficiency by a small kinetic impactor", Journal of Spacecraft and Rockets, Vol. 50, No. 2, Mar.–Apr. 2013, pp. 380-393, doi: 10.2514/1.A32304, ISSN 0022-4650.

[4] Payez A., Shoenmaekers J., "Parameter-space study of kinetic-impactor mission design", 5th Planetary Defense Conference (PDC 2017), Tokyo, May 15–19 2017.

[5] Thiry N., Vasile M., "Statistical multicriteria evaluation of asteroid deflection methods", 67th International Astronautical Congress, Guadalajara, Mexico, 26-30 September 2016.

[6] Opik, E. J., "Collision Probabilities with the Planets and the Distribution of Interplanetary Matter," Proceedings of the Royal Irish Academy. Section A: Mathematical and Physical Sciences, Vol. 54, 1951, pp. 165-199.

[7] Bottke, W. F., Morbidelli, A., Jedicke, R., Petit, J.-M., Levison, H. F., Michel, P. and Metcalfe, T. S., "Debiased Orbital and Absolute Magnitude Distribution of the near-Earth Objects," Icarus, Vol. 156, No. 2, 2002, pp. 399-433. doi: 10.1006/icar.2001.6788

[8] http://newton.dm.unipi.it/neodys/ [Last accessed 04/09/2017]

[9] https://cneos.jpl.nasa.gov/sentry/ [Last accessed 04/09/2017]

[10] W.J. Larson, J.R. Wertz, Space Mission Analysis and Design, Third Ed., Kluwer Academic Publishers, Boston, USA, 2005.

[11] Ariane Group, http://www.space-propulsion.com/spacecraft-propulsion/hydrazine-thrusters/20n-hydrazine-thruster.html, access on 05/09/2017

[12] Mitsubishi Precision Company, Limited, Kamakura-city, Kanagawa Prefecture, Japan, http://www.mpcnet.co.jp/e/index.html

[13] R. Biesbroek, Lunar and Interplanetary Trajectories, Springer, UK, Praxis Publishing Chichester, 2016